

Kinetics of Chlorine Atom Reaction with Hydrogen Bromide

Otto Dobis and Sidney W. Benson*

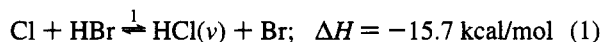
Loker Hydrocarbon Research Institute, University of Southern California, University Park, Los Angeles, California 90089-1661

Received: October 21, 1994; In Final Form: January 3, 1995*

The kinetics of reaction $\text{Cl} + \text{HBr} \xrightarrow{1} \text{HCl}(\nu) + \text{Br}$ have been studied at 298 K using the very low pressure reactor (VLPR). $k_1 = (6.16 \pm 0.07) \times 10^{-12} \text{ cm}^3/(\text{molecule s})$, calculated from both the reactant consumption and Br product formation rate measurements. Mass conservation is found to be $97 \pm 3\%$ for the overall chemical change in the system. Calculations using known relaxation rates for $\text{HCl}(\nu)$ show that vibrationally excited products of either $\text{HCl}(\nu=2)$ or $\text{HBr}(\nu=1)$ have no measurable contribution to the kinetics of reaction 1 under the steady-state flow conditions in the VLPR system.

Introduction

The relatively fast and highly exothermic hydrogen exchange of halogen atoms with hydrogen halides has provided an important class of chemical reactions for experimental and theoretical investigation of detailed, state-to-state reaction dynamics.^{1–3} The title reaction



produces vibrationally excited HCl up to the $\nu = 2$ level but no electronically excited Br atom in the primary process.⁴ The significance of this apparently simple reaction is that it constitutes the pumping stage of pulsed Cl + HBr chemical laser,⁵ and the rate constant k_1 , as well as the initial vibrational and rotational (ν, J) distributions, are the input parameters for the laser gain calculation. The same accurate data are needed for checking trajectory calculations applied to the microscopic reversibility dynamics of this heavy–light–heavy type exoergic exchange reaction. But unfortunately, all these data, especially the rate constant of reaction 1 obtained with different experimental techniques, show a surprising spread in values.

k_1 values range from 3.8×10^{-12} to $1.1 \times 10^{-11} \text{ cm}^3/(\text{molecule s})$ at room temperature.^{6–13} The lowest value⁶ has been obtained in our laboratories using the very low pressure reactor (VLPR) experimental system in its early stage of development. Therefore, we report here the reinvestigation of reaction 1 using the recently developed kinetic versatility of the VLPR system.^{14,15} The use of this improved experimental technique allows us to measure the rates of both the reactant consumption and product formation under real second-order conditions, providing thereby an excellent mass conservation cross-check. We vary the concentrations of reactants and their ratios over a wide range and change the residence time of the steady-state flow by changing the escape orifice size of the reactor vessel. Such a “multiparametric” chemical kinetic investigation provides reliable rate constant accompanied with mass balance measurements that establish all chemical changes occurring in the system.

The relative vibrational energy distribution of HCl product is known from cold-wall arrested-relaxation³ and fast-flow afterglow¹⁶ measurements for the ν_1/ν_2 ratio. Reported data give a most probable relative population¹² of $\nu_0:\nu_1:\nu_2 = 0.32:0.49:0.19$, in good agreement with linear surprisal analysis. This internal energy distribution is the basis of kinetic investigations

measuring the time dependence of infrared chemiluminescence intensity^{7–10,12} of $\text{HCl}(\nu)$ product formed after the initiation of reaction 1 with a UV laser pulse in the Cl_2/HBr system. Since the excited $\text{HCl}(\nu=2)$ product may enhance the back-reaction -1^* or induce certain undesirable side reaction triggered by collisional relaxation, we have examined their effects and found that they do not contribute significantly to our measurements of k_1 .

Experimental Section

The three-stage, all turbo-pumped VLPR system used in earlier kinetic investigations^{14,15,17} was utilized in the present study.

A thin-Teflon-coated, cylindrical, thermostated reactor cell of volume $V_r = 217.5 \text{ cm}^3$ (diameter 4.7 cm) is mounted on the top of the main vacuum chamber. The reactor base is seated on a Teflon-coated, rapidly adjustable slide¹⁸ having three interchangeable escape orifices with diameters of 0.193, 0.277, and 0.485 cm. Their use in different runs is indicated as ϕ_2 , ϕ_3 , and ϕ_5 , respectively, in Tables 1 and 2 and marked with different symbols in Figures 2 and 3. With this reactor volume, the unimolecular escape rate constants for gas components of mass M are given by $k_{eM} = a_\phi(T/M)^{1/2} \text{ s}^{-1}$, where T is the absolute temperature and $a_\phi = 0.258$ for ϕ_2 , 0.546 for ϕ_3 , and 1.321 for ϕ_5 orifices.¹⁸ With a surface area of about 222 cm^2 there will be about 7600 wall collisions for a_2 , 3700 for a_3 , and 1200 for a_5 apertures before escape from the reactor. Wall collisions are generally 100–1000-fold more frequent than reactive collisions in the systems studied.

Gas inlets are located at the top of the reactor cell. They are connected to separate capillary flow subsystems calibrated for regulating the fluxes of initial gas components with the use of Validyne transducers.¹⁸ The Cl_2 flow traverses a H_3PO_4 -coated quartz discharge tube centered in the microwave cavity of a McCarroll antenna at the inlet of the reactor cell.

Gas leaving the reactor cell through a selected exit orifice is collimated into a molecular beam by two successive pinholes in the differentially pumped vacuum system. This beam is chopped by a tuning fork and sampled with an off-axis mass analyser of a BALZERS QMG 511 quadrupole mass spectrometer. The signal is fed to a phase-sensitive lock-in amplifier and chart recorded. The mass range of interest is repeatedly scanned, usually 20–25 times to give a good statistical average, and the mass intensities are recorded. Each mass signal is corrected for its background value (usually small) recorded prior to the start-up of mass flow.

* Abstract published in *Advance ACS Abstracts*, March 15, 1995.

VLPR depends on avoiding back-diffusion from the reactor to either the upstream gases or the microwave discharge region. This is accomplished by fixing the conductances from both of these regions into the reactor to be less than the conductance of the smallest exit aperture (ϕ_2).

The mass spectrometer signal is proportional to the steady-state concentration of a species in the reactor. This in turn is proportional to the flux of that species in the system. Mass spectral calibrations for each gas component are carried out by measuring the mass signal intensity (I_M) as a function of the specific flux $F(M)$ according to the relationship $I_M = \alpha_M F(M)$, where α_M is the mass spectral efficiency for mass M and $F(M) = (\text{flux})/V_r$ in molecules/(cm³ s). The steady-state concentration of the gas component M in the reactor cell then can be calculated from the relation $[M] = F(M)/k_{eM}$ (molecules/cm³).

Initially, the Cl₂ flow is started using 4.5% Cl₂/He mixture (both are Matheson research grade gases). The mass range $m/e = 69-75$ is repeatedly scanned using 20 V electron energy. $m/e = 70, 72$, and 74 are used as a Cl isotope composition check. The signal intensity of $m/e = 70$ is also used for checking the constancy in time of the mass spectral efficiency α_{Cl_2} .

Next, the microwave power is turned on, and the power is adjusted to 100% breakup of Cl₂ as witnessed by the disappearance of Cl₂ mass signals. Cl atom production is always accompanied by some HCl formation, presumably from Cl reaction with H₃PO₄ on the wall of the microwave discharge tube. Mass range 34–39 is scanned, and since HCl fragmentation into Cl⁺ is negligibly small (0.24%) at 20 V electron energy and $\alpha_{Cl} = \alpha_{HCl}$,¹⁴ the Cl and HCl concentrations can be calculated from the recorded mass signal intensities of $m/e = 35$ and 36 (and also from their isotopic species at mass 37 and 38) as given in column 2 of Table 1. The initial steady-state concentration of Cl can now be calculated as $[Cl]_0 = 2F(Cl_2) - F_{Cl}/(F_{Cl} + F_{HCl})k_{eCl}$ (column 3 of Table 1). The Cl concentration can be further checked by adding a reactant RH such as C₂H₆ and showing that the HCl produced is equal to $\Delta[Cl]$, the change in the measured Cl concentration.

After having established the initial $[Cl]_0$ and $[HCl]_0$ concentrations, the flow of pure HBr (Matheson, 99.8% purity, further purified by trap-to-trap vacuum distillation) is started up and increased until a sizable decrease of Cl mass signal is achieved. Mass range 34–39 is scanned again, and the new values of $[Cl]$ and $[HCl]$ are calculated (columns 4 and 5 of Table 1). Then, the mass spectrometer is turned to scan the mass range of $m/e = 78-83$ using both 20 V and the more sensitive 40 V electron energies. These mass spectral intensities are proportional to the steady-state concentrations of Br and HBr using the signals of both ⁷⁹Br and ⁸¹Br isotopes.

Mass ranges of 113–119 and 157–163 were also checked for possible traces of BrCl and Br₂ recombination products formed during the run of reaction 1. No detectable signal increase of those masses over their background values was observed. Note that any oil or hydrocarbon impurities would contribute easily observable HBr and HCl peaks. None are observed.

Results

VLPR is a genuine steady-state system in which mixing by molecular diffusion can be shown to be complete in less than 0.1% of the residence time of the species in the system. Hence, all kinetic equations reduce the algebraic equations, reflecting this steady-state condition. These equations are all first order in the rate constants; hence, measurements of the steady-state concentrations of reactants and products can yield all the rate constants involved.

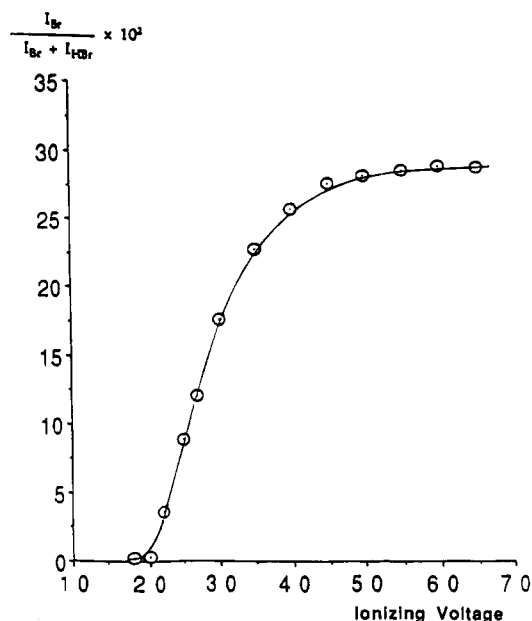


Figure 1. Fragmentation ratio of Br⁺ produced by HBr⁺ fragmentation as a function of applied ionizing electron energy in the quadrupole mass analyzer. Data are recorded with 2.51×10^{12} molecule/(cm³ s) specific flow of HBr.

The steady-state condition of Cl atom consumption according to reaction 1 and the reactor escape process lead to exact kinetic equations

$$\frac{\Delta[Cl]}{[Cl]}k_{eCl} = \frac{\Delta[HCl]}{[Cl]}k_{eHCl} = k_1[HBr] \quad (2)$$

where $\Delta[Cl] = [Cl]_0 - [Cl]$, the difference of the initial and final Cl atom concentrations. Similarly, the steady-state kinetics of Br atom formation gives

$$\frac{[Br]}{[Cl]}k_{eBr} = \frac{\Delta[HBr]}{[Cl]}k_{eHBr} = k_1[HBr] \quad (2a)$$

Although $[Cl]_0$ and $[Cl]$ concentrations measured with 20 eV electrons are directly proportional to the measured mass spectral intensities of Cl atom, Br and HBr signals must be corrected for HBr fragmentation of the electron energies used.

The mass fragmentation pattern of HBr measured with $F(HBr) = 2.514 \times 10^{12}$ molecules/(cm³ s) specific flow rate is presented in Figure 1. At the two ion electron voltages employed for HBr and Br, the fragmentation ratios were measured by varying the HBr flow rate in the range $(1.07-15.78) \times 10^{12}$ molecules/(cm³ s). The observed ratios of $10^2 I_{Br}/(I_{Br} + I_{HBr})$ are 0.30 ± 0.08 at 20 V and 25.64 ± 0.19 with 40 V mass spectrometry. In these measurements both stable isotopes of Br were used, and the averages of the measured data are displayed in Figure 1. The ⁷⁹Br isotope composition calculated from our mass spectroscopic analysis is $50.52 \pm 0.43\%$. It is in precise agreement with the *Chemical Handbook* value of standard natural abundance for ⁷⁹Br/⁸¹Br isotopes.

Mass signal intensities of $m/e = 79$ and 80 , as well as 81 and 82 , recorded in reaction 1 with both 20 and 40 V electron energies were corrected using the above fragmentation ratios, respectively, and the average of Br/HBr conversion calculated for each run is given in column 6 of Table 1. The scatter indicates that the accuracy is better than 1%. Corrections for fragmentation with 20 V measurements are small but significant at low conversion of HBr. Steady-state concentrations of Br and HBr calculated from the flow rate of $F(HBr)_0$ using the

TABLE 1: Initial Concentrations^a of Cl and the Final Steady-State Concentrations of Reactants and Products Measured in the Experimental Runs

no./ ϕ_s	$I_{\text{Cl}}^0/(I_{\text{Cl}}^0 + I_{\text{HCl}}^0) \times 10^2$	$[\text{Cl}]_0$	$I_{\text{Cl}}/(I_{\text{Cl}} + I_{\text{HCl}}) \times 10^2$	$[\text{Cl}]$	$I_{\text{Br}}/(I_{\text{Br}} + I_{\text{HBr}}) \times 10^2$	$[\text{Br}]$	$[\text{HBr}]$	ΣP_i^b
1/ ϕ_2	47.28	16.542	18.58	6.502	87.65 ± 0.45	14.866	2.108	0.55
2/ ϕ_2	47.28	16.545	9.81	4.315	84.03 ± 0.47	20.772	3.973	0.57
3/ ϕ_2	56.68	20.300	8.46	2.961	76.51 ± 0.47	25.923	8.010	0.61
4/ ϕ_3	53.08	9.671	16.49	2.936	62.71 ± 0.76	10.015	5.993	0.31
5/ ϕ_3	60.32	10.990	9.02	1.606	47.85 ± 0.44	14.043	15.402	0.35
6/ ϕ_3	60.32	10.990	6.20	1.104	40.08 ± 0.41	15.527	23.360	0.39
7/ ϕ_5	42.83	3.211	26.50	1.998	31.77 ± 0.46	1.890	4.085	0.13
8/ ϕ_5	55.02	4.148	27.31	2.059	31.46 ± 1.00	2.763	6.057	0.13
9/ ϕ_5	55.82	4.208	20.17	1.521	26.46 ± 0.34	4.241	11.8620	0.16
10/ ϕ_5	58.55	4.414	17.00	1.282	23.03 ± 1.03	4.706	15.827	0.17

^a All concentrations are in units of 10^{11} particles/cm³. ^b ΣP_i is the total pressure in mTorr units of the system calculated from steady-state concentrations including HCl and He, too.

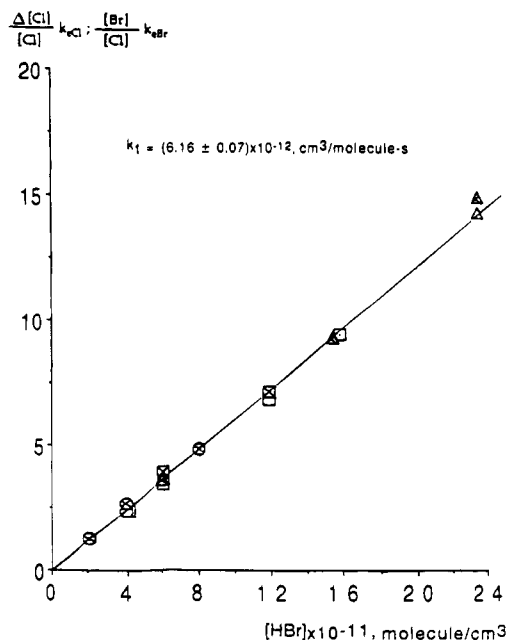


Figure 2. Dependence of relative Cl atom consumption and Br atom formation on the steady-state concentration of HBr according to kinetic equations (2), open symbols, and (2a), crossed symbols, at 298 K. Symbols indicating the orifices used for given data pairs: \circ , ϕ_2 ; Δ , ϕ_3 ; \square , ϕ_5 .

escape rate constants of the selected discharge orifice are given in columns 7 and 8 of Table 1, respectively.

Concentrations measured in 10 different runs are presented in Figure 2 plotted according to eqs 2 and 2a. Crossed symbols mark the data calculated from $[\text{Br}]$ formation kinetics. All the data lie on the same straight line passing through the origin. This indicates the absence of any surface reaction. The slope gives the rate constant of reaction 1 as

$$k_1 = (6.16 \pm 0.07) \times 10^{-12} \text{ cm}^3/(\text{molecule s})$$

Combination of eqs 2 and 2a gives the mass balance equation

$$\Delta[\text{Cl}]k_{\text{eCl}} = [\text{Br}]k_{\text{eBr}} \text{ or } \Delta[\text{HBr}]k_{\text{eHBr}} = [\text{Br}]k_{\text{eBr}} \quad (3)$$

for the Cl atom consumption and Br atom product formation. Figure 3 shows that the overall chemical change in the system corresponds to reaction 1, and its kinetics can be described with $97.0 \pm 3.0\%$ accuracy using VLPR.

Discussion

An important feature of being able to measure both products and reactants is that we can obtain accurate rate constants at

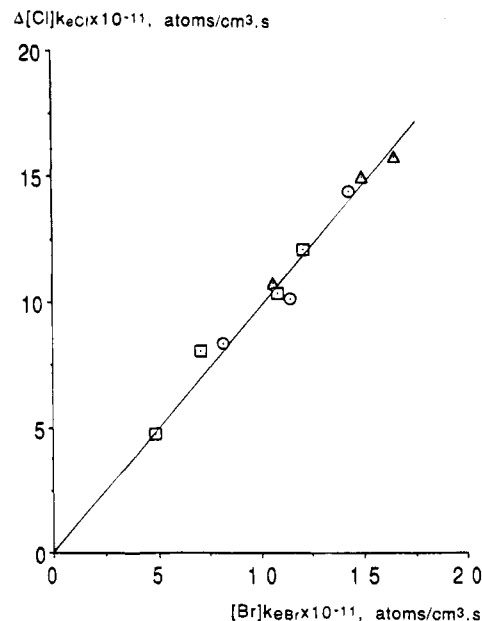
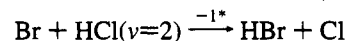


Figure 3. Flow balance between Cl atom consumption and Br atom product formation according to eq 3. Symbols of orifices are the same as in Figure 2.

low consumptions of reactants from the observed products and at high conversions of reactants from the changes in the reactant concentrations.

The highly accurate measurement of the overall chemical change in the VLPR system is not surprising. We have achieved similar accuracy in even more complicated systems^{14,17} since the simultaneous mass analysis of reactant consumption and product formation was introduced. The observed excellent balance is found over the entire range of concentration changes. The HBr conversion (Table 1) is varied between 23% and 87%. However, whether or not the kinetics of this chemical change can be described with one single thermal rate constant k_1 when vibrationally excited products are present in the system still needs to be examined. It has been suggested^{12,13} that the energized back-reaction



$$k_{-1}^* = 1.46 \times 10^{-12} \text{ cm}^3/(\text{molecule s})^{19}$$

may reduce the measured value of the forward rate constant under real second-order conditions. The same back-reaction with $\text{HCl}(\nu=1)$ is negligible as its rate constant is 45 times smaller^{19,20} than our measured rate constant k_1 .

The authors, however, have completely overlooked the long time scale for VLPR experiments. The typical HCl molecule

TABLE 2: Steady-State Distributions of HCl($v=2$) Product and HBr($v=1$) Reactant and Their Effect on the Kinetics of Cl + HBr Reaction^a

no./ ϕ_x	$[\text{HCl}]_{v_2} \times 10^{-10}$, molecules/cm ³	$k^*_{-1}([\text{HCl}]_{v_2}/k_{\text{eBr}}) \times 10^2$	$([\text{HBr}]_{v_1}/[\text{HBr}]) \times 10^2$	$(1 + k^*_{-1}[\text{HCl}]_{v_2}/k_{\text{eBr}})/(1 - ([\text{HBr}]_{v_1}/[\text{HBr}])(1 - k'_1/k_1))$
1/ ϕ_2	1.083	2.85	2.083	0.997
2/ ϕ_2	1.166	3.09	2.652	0.991
3/ ϕ_2	1.319	3.49	4.633	0.968
4/ ϕ_3	1.808	2.49	2.545	0.987
5/ ϕ_3	1.825	2.52	4.488	0.961
6/ ϕ_3	1.638	2.26	4.796	0.954
7/ ϕ_5	1.343	0.76	0.989	0.993
8/ ϕ_5	1.680	0.98	1.340	0.990
9/ ϕ_5	1.961	1.12	1.660	0.987
10/ ϕ_5	1.960	1.12	2.166	0.979

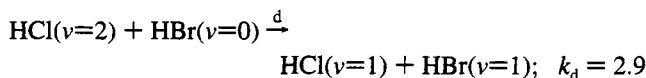
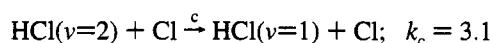
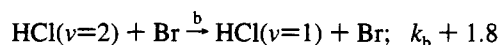
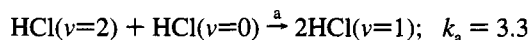
^a This neglects the considerable effect of spontaneous emission by these species and so must be looked upon as upper limits in the ϕ_5 experiments and much smaller in ϕ_2 and ϕ_3 experiments.

in our system escapes with a unimolecular rate constant of about 0.82 s^{-1} (ϕ_2), 1.6 s^{-1} (ϕ_3), or 3.8 s^{-1} (ϕ_5). These are all long compared to the rate constant of spontaneous emission of HCl($v=2$) or HCl($v=1$), which are 59.5 and 34.6 s^{-1} , respectively. Hence, the steady-state population of excited HCl in our system is less than 1% of ground state HCl even in the absence of any quenching. However, we have calculated the effect of quenching in the absence of spontaneous emission and will show that quenching alone is sufficient to reduce HCl(v) to negligible proportions.

The competing reaction for HCl($v=2$) emission is the reverse reaction with Br. With $k^*_{-1} \approx 1.5 \times 10^{-12} \text{ cm}^3/(\text{molecule s})$ (ref 19) and a mean value of $[\text{Br}] = 1 \times 10^{12} \text{ atoms/cm}^3$ (Table 1), the mean rate of loss of HCl($v=2$) by step -1^* is 1.5 s^{-1} or about 2.5% of the radiation loss and thus negligible in its effect in the measure of k_1 .

Similarly, the spontaneous emission from HBr($v=1$)²⁹ in our system of 7.3 s^{-1} together with the negligible concentrations of HCl($v=2$) or HCl($v=1$) needed to excite it make vibrational effects unimportant in VLPR studies. This is an important difference from flash photolysis or flow systems^{7-10,12,13} where just the opposite is true.

It is known that the thin Teflon coating of our reactor cell is chemically inert. No atom loss due to wall removal is observed as demonstrated by Cl and Br atom conservation measurements.¹⁴ No such test can be performed for the effectiveness of vibrational relaxation by collisions with the Teflon-coated wall. However, there is a compilation²¹ on the rate of gas phase vibrational relaxation of HCl($v=2$) by collisions with a number of different atoms and molecules including those being present in our system. These are (in units of $10^{-12} \text{ cm}^3/(\text{molecule s})$)



The most effective collisional partner is HCl($v=0$), which is always present in excess in our system, since about half of the inlet Cl_2 is converted into HCl in the microwave discharge tube. Taking the initial relative vibrational population of HCl given in the Introduction and the concentration values of Table 1, the

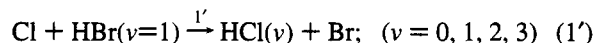
steady-state concentration of HCl($v=2$) can be calculated as

$$[\text{HCl}]_{v_2} = 0.19k_1[\text{Cl}][\text{HBr}]/(k_a\{[\text{Cl}]_0 + 0.32\Delta[\text{Cl}]\} + (k_b + k^*_{-1})[\text{Br}] + k_c[\text{Cl}] + k_d[\text{HBr}] + k_{\text{eHBr}}) \quad (4)$$

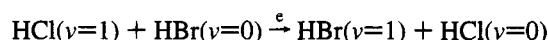
where $[\text{Cl}]_0 + 0.32\Delta[\text{Cl}] \sim [\text{HCl}]_{v_0}$ with the approximation of $[\text{Cl}]_0 \sim [\text{HCl}]_0$ (see column 2 of Table 1). The calculated HCl($v=2$) steady-state concentration is small in each run, as shown in column 2 of Table 2.³⁰

Incorporating reaction -1^* into the mechanism, a multiplication factor of $1 + k^*_{-1}[\text{HCl}]_{v_2}/k_{\text{eBr}}$ for the right side of eqs 2 and 2a can be derived. As can be seen from the data in column 3 of Table 2, the deviation of this factor from the unity is, though slightly orifice dependent, small and contributes only a 2% increase in the reported k_1 value on average.

From a kinetic point of view, the rate enhancement of HBr($v=1$) according to the reaction



may also be of interest. Vibrationally excited HBr is produced in V-V transfer (d) and in



$$k_e = 1 \times 10^{-12} \text{ cm}^3/(\text{molecule s})^{20}$$

transfer process. The rate constant of reaction $1'$ is not known from experimental investigation. Quasi-classical trajectory calculation²³ gives the ratio of $k'_1/k_1 = 2.5$ at 298 K. Since this theoretical study selects the London-Eyring-Polanyi-Sato (LEPS) potential surface parameters to match with a higher k_1 value, we adopt the ratio of 2.5 only to our measured k_1 to estimate $k'_1 = 1.54 \times 10^{-11} \text{ cm}^3/(\text{molecule s})$. With this rate constant k'_1 , an equation for the relative steady-state concentration of vibrationally excited HBr produced in V-V transfers (d) and (e):

$$\frac{[\text{HBr}]_{v_1}}{[\text{HBr}]} = \frac{k_d[\text{HCl}]_{v_2}}{k_1[\text{Cl}] + k_{\text{eHBr}}} \left[1 + \frac{k_e/k_d}{k_e[\text{HBr}] + k_{\text{eHCl}}} (2k_a[\text{HCl}]_{v_0} + k_b[\text{Br}] + k_c[\text{Cl}] + k_d[\text{HBr}]) \right] \quad (5)$$

can be derived.²⁴ This ratio varies between 1% and 4.5% in the experimental runs as shown in column 4 of Table 2.

Inclusion of reaction $1'$ into the mechanism results in a factor of $\{1 - (1 - k'_1/k_1)[\text{HBr}]_{v_1}\}^{-1}$ for the right side of eqs 2 and 2a, and the steady-state kinetics for the overall mechanism including reactions 1, -1^* , and $1'$ is now given by the equation

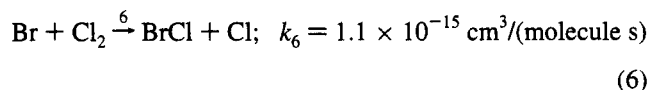
$$\frac{\Delta[\text{Cl}]}{[\text{Cl}]} k_{\text{eCl}} \frac{1 + k_{-1}^*[\text{HCl}]_{\text{v}_2}/k_{\text{eBr}}}{1 - (1 - k_{-1}^*/k_1)[\text{HBr}]_{\text{v}_1}/[\text{HBr}]} = k_1[\text{HBr}] \quad (2c)$$

The correction factor due to reactions -1^* and $1'$ is slightly less than 1, that is, 0.981 ± 0.015 on average, as shown in column 5 of Table 2. If it were significant, a negative intercept with $[\text{HBr}] = 0$ in Figure 2 would have appeared. The regression on the linear function of Figure 2 gives $(-8.03 \pm 7.75) \times 10^{-2}$ for the intercept, indicating that the small experimental scatter overrides the deviation caused by the correction factor of the extended mechanism. On the basis of the above evaluation, we conclude that *vibrationally excited products of either $\text{HCl}(\text{v}=2)$ or $\text{HBr}(\text{v}=1)$ make no measurable contribution to the kinetics of reaction 1 under the steady-state flow conditions in the VLPR system.*

The earlier VLPR study⁶ of reaction 1 was done in a narrow range of reactant concentrations using 30 V electron energy without taking proper corrections for mass fragmentations. Figure 1 shows that the HBr fragmentation is 17.6% and the HCl fragmentation²⁵ is close to 4% with 30 eV electrons. Corrections for these mass fragmentations will increase the reported rate constant⁶ to $\sim 6 \times 10^{-12} \text{ cm}^3/(\text{molecule s})$, very close to the present value.

The highest reported rate constant¹¹ $k_1 = 11 \times 10^{-12} \text{ cm}^3/(\text{molecule s})$ was measured with a competitive experimental technique using the first step H abstraction of $\text{Cl} + \text{C}_2\text{H}_6$ reaction as standard. Since the conversion of C_2H_6 was set between 55% and 85% and all secondary reactions of ethyl radicals were neglected, this study may incur a serious error. We are currently using this combined system to study the reactions of ethyl radicals with HBr and Br. Applying the same oversimplified competition scheme¹¹ to our preliminary experiments in the same high conversion range of C_2H_6 , we could reproduce that high rate constant value, but with discernible defect in mass conservations of Cl and C_2H_6 .

Another high value of $k_1 = 10 \times 10^{-12} \text{ cm}^3/(\text{molecule s})$ is obtained with time-resolved infrared chemiluminescence measurements¹² of $\text{HCl}(\text{v}=2)$ product emission after laser pulse initiation of reaction 1 in the Cl_2/HBr system. The time-dependent $\text{HCl}(\text{v}=2)$ emission intensity is recorded in competition with V-V relaxation process d. Calculation of rate constant k_1 would require the knowledge of initial $\text{HCl}(\text{v}=2)$ distribution and Cl atom concentration, but for the intensity ratios of the steady-state and initial IR emissions, these two parameters can be substituted for the rate of the consecutive slow chain reaction

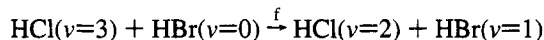


with apparently reasonable kinetic approximations. Rate constant k_6 is then obtained from measurements using different Cl_2/HBr ratios. The mechanism involving reactions 1, 6, and d, together with conditional limitations, constitutes a very complicated kinetic system most likely resolvable when the emission of the highest vibrationally populated product state is recorded and the rate constant of reaction 6 is above a certain low limit. Instead of going into detailed discussions, we would like to point out that the reported kinetic data do not fit well to the proposed mechanism as it can be disclosed by the relatively large intercept, about 35% of the steady-state/initial intensity ratios in Figure 6 of ref 12. Such a deviation may arise from the contribution of reaction $1'$. Although the average consumption of HBr is kept around 3% in reaction 1 to facilitate the pseudo-first-order condition, neither -1^* nor $1'$ has any appreciable

influence on the overall rate, but as expected, if the HCl product of reaction $1'$ has a different vibrational distribution, it should be accounted for in the kinetics.

In order to measure k_1 from observations of the IR emission from $\text{HCl}(\text{v}=2)$, an accurate knowledge of the quenching rate by HBr is needed. The two are occurring on the same time scale. In order to minimize this, the authors determine k_1 from very early-time measurements ($< 10^{-5} \text{ s}$). Unfortunately, the HCl produced in reaction 1 is both vibrationally and rotationally excited. To use the data, it is assumed that rotational relaxation to a thermal distribution has occurred. It takes about 10–100 collisions to rotationally relax HX type molecules. The only good rotational relaxer present is HBr ($\sim 10^{15}/\text{cm}^3$). In 10^{-5} s the average $\text{HCl}(\text{v}=2)$ will make 2.5 collisions. This is not enough for rotational relaxation! Such relaxation must be verified. The same situation holds for $\text{HCl}(\text{v}=1)$.

The vibrational distribution of HCl produced in reaction $1'$ is not known from experimental measurements. However, for the product partitioning of the available energy in reaction $1'$, Brown et al.²⁶ have derived a distribution of $v_0:v_1:v_2:v_3 = 0.11:0.30:0.35:0.24$ in a Monte Carlo aided quasi-classical trajectory study of reaction 1. Here not only is the $\text{HCl}(\text{v}=2)$ population nearly doubled, but $\text{HCl}(\text{v}=3)$ product also appears in a high ratio that then cascades to $\text{HCl}(\text{v}=2)$ according to



Rate constant k_f is not known, but process f is presumably faster than process d. Propagations of reaction $1'$ and process f on the experimental time scale may result in 20–30% increase at the limiting steady-state intensity of $\text{HCl}(\text{v}=2)$.

Reaction $1'$ produces $\text{HCl}(\text{v}=1)$ in a lower proportion than reaction 1. It may explain in part the experimental discrepancy that k_1 obtained from the time-resolved IR radiation of filtered $\text{HCl}(\text{v}=1)$ emission is half that measured with recording $\text{HCl}(\text{v}=2)$ intensity¹² in the same experimental system using different band filters.

Other Cl_2/HBr laser-initiated chemiluminescence kinetic studies^{7–10} are done recording the time-resolved IR emission of all vibrationally excited states of $\text{HCl}(\text{v}>0)$ product and reporting k_1 values between 7.4×10^{-12} and $8.5 \times 10^{-12} \text{ cm}^3/(\text{molecule s})$ at 300 K. Here the influence of reaction $1'$ is less significant as its excess vibrational emission is averaged over a broader spectrum than in the case of $\text{HCl}(\text{v}=2)$ analysis. However, it may still account for a 10–15% increase in k_1 value as it can be traced, beyond a relatively large scatter, in the slight decrease of k_1 with increasing HBr pressure in Figure 3 of ref 7.

The above discussion points to the need of further refinement of the chemiluminescence method concerning the exact source of excited HCl product and its changing rotational and vibrational distribution on the reaction time scale.

Time-resolved Cl atom fluorescence measurements¹³ with laser pulse initiation of reaction 1 in the Cl_2/HBr system diluted with N_2 give $k_1 = (5.9 \pm 0.15) \times 10^{-12} \text{ cm}^3/(\text{molecule s})$, where side reactions -1^* and $1'$ are insignificant due to the pseudo-first-order condition for HBr concentration. Our measured k_1 value well agrees with that within the noted uncertainty. This is an excellent technique to study the kinetics of reaction 1 with only minor potential degradation of the 135–140 nm Cl atom fluorescence emission at large excess HBr concentrations ($\alpha_{\text{HBr}} \sim 6 \times 10^{-19} \text{ cm}^2$ in that wave band²⁷). Such concern with the use of Cl atom fluorescence technique was recently noted.²⁸

The temperature dependence of k_1 , the investigation of which is under progress in our laboratories, is also a matter of controversy. Some works report a normal Arrhenius behavior

with $E_{\text{act}} = 0.9^{11}$ and $0.8 \text{ kcal/mol}^{13}$ while the $\text{HCl}(\nu > 0)$ chemiluminescence measurements⁹ exhibit a non-Arrhenius behavior especially over 300 K. If the relative rotational population of $\text{HCl}(\nu > 0)$ vibrational states decreases with increasing temperature as suggested by Brown et al.,²⁶ the concave curvature of $\ln k_1$ with $1/T$ might be anticipated. Concave curvature of an Arrhenius plot to the $1/T$ axis has no known physical explanation but can be evidence for a complex contribution from more than one chemical reaction.

Conclusions

The reaction of $\text{Cl} + \text{HBr}$ was investigated using measurements of all reactants and products under steady-state flow conditions in the VLPR system. Both the reactant consumption and Br product formation rates give the same rate constant with $97.0 \pm 3.0\%$ mass conservation.

Taking account of spontaneous emission and of the vibrational relaxation of nascent excited HCl product, it is shown that neither the back-reaction -1^* of $\text{HCl}(\nu=2)$ nor the excited HBr ($\nu=1$) forward reaction $1'$ has any measurable effect on our observed rate of reaction 1 under steady-state conditions. The kinetics can thus be completely described with one thermal rate constant. Our measured rate constant $k_1 = (6.16 \pm 0.07) \times 10^{-12} \text{ cm}^3/(\text{molecule s})$ at 298 K is in good agreement with the reported value¹³ measured with time-resolved Cl atom resonance fluorescence technique, but it is lower by a factor of 1.3–1.7 than those obtained by using time-resolved chemiluminescence spectrometry of $\text{HCl}(\nu > 0)$ product.^{7–10,12} It is pointed out that reaction $1'$ may enhance the vibrational population of $\text{HCl}(\nu)$ product, especially that of $\text{HCl}(\nu=2)$ on the time scale of recorded chemiluminescence, thereby leading to some overestimate of k_1 .

Acknowledgment. This work has been supported by a grant from the National Science Foundation (CHE-87-1467) and a gift from the Occidental Petroleum Co.

References and Notes

- (1) Kuntz, P. J.; Nemeth, E. M.; Polanyi, J. C.; Rosner, S. D.; Young, C. E. *J. Chem. Phys.* **1966**, *44*, 1168.

- (2) Maylotte, D. H.; Polanyi, J. C.; Woodall, K. B. *J. Chem. Phys.* **1972**, *57*, 1547.
- (3) Douglas, D. J.; Polanyi, J. C.; Sloan, J. J. *J. Chem. Phys.* **1976**, *13*, 15.
- (4) Anlauf, K. G.; Horne, D. S.; Macdonald, R. G.; Polanyi, J. C.; Woodall, K. B. *J. Chem. Phys.* **1972**, *57*, 1561. Bly, S. H. P.; Brandt, D.; Polanyi, J. C. *J. Chem. Phys. Lett.* **1979**, *65*, 399.
- (5) Airey, J. R. *J. Chem. Phys.* **1970**, *52*, 156. Keren, E.; Gerber, R. B.; Ben-Shaul, A. *J. Chem. Phys.* **1976**, *21*, 1.
- (6) Lamb, J. J.; Kondo, O.; Benson, S. W. *J. Phys. Chem.* **1986**, *90*, 914.
- (7) Wodarczyk, F. J.; Moore, C. B. *J. Chem. Phys. Lett.* **1974**, *26*, 484.
- (8) Bergman, K.; Moore, C. B. *J. Chem. Phys.* **1975**, *63*, 643.
- (9) Mei, C. C.; Moore, C. B. *J. Chem. Phys.* **1977**, *67*, 3936.
- (10) Nesbitt, D. J.; Leone, S. R. *J. Chem. Phys.* **1981**, *75*, 4949.
- (11) Rubin, R.; Persky, A. *J. Chem. Phys.* **1983**, *79*, 4310.
- (12) Dolson, D. A.; Leone, S. R. *J. Phys. Chem.* **1987**, *91*, 3543.
- (13) Nicovich, J. M.; Wine, P. H. *Int. J. Chem. Kinet.* **1990**, *22*, 379.
- (14) Dobis, O.; Benson, S. W. *J. Am. Chem. Soc.* **1991**, *113*, 6377.
- (15) Dobis, O.; Benson, S. W.; Mitchell, T. J. *J. Phys. Chem.* **1974**, *98*, 12284.
- (16) Wickramaaratchi, M. A.; Setser, D. W. *J. Phys. Chem.* **1983**, *87*, 64.
- (17) Dobis, O.; Benson, S. W. *J. Am. Chem. Soc.* **1993**, *115*, 8798.
- (18) Dobis, O.; Benson, S. W. *Int. J. Chem. Kinet.* **1987**, *19*, 691.
- (19) Golden, D. M.; Spokes, G. N.; Benson, S. W. *Angew. Chem., Int. Ed. Engl.* **1973**, *12*, 534.
- (20) Arnoldi, D.; Kaufmann, K.; Wolfrum, J. *Phys. Rev. Lett.* **1975**, *34*, 1597.
- (21) Leone, S. R.; Macdonald, R. G.; Moore, C. B. *J. Chem. Phys.* **1975**, *63*, 4735.
- (22) Leone, S. R. *J. Phys. Chem. Ref. Data* **1982**, *11*, 953.
- (23) Leone, S. R.; Moore, C. B. *J. Chem. Phys. Lett.* **1973**, *19*, 340.
- (24) Broida, M.; Persky, R. *J. Chem. Phys.* **1989**, *133*, 405.
- (25) For the derivation of eq 5, we employed the steady-state concentration of $\text{HCl}(\nu=1)$ set by V–V processes a–e as

$$[\text{HCl}]_{\nu=1} = \frac{2k_a[\text{HCl}]_{\nu=0} + k_b[\text{Br}] + k_c[\text{Cl}] + k_d[\text{HBr}]}{k_e[\text{HBr}] + k_{\text{eHCl}}}$$

- (26) Dobis, O.; Benson, S. W. *J. Am. Chem. Soc.* **1990**, *112*, 1023.
- (27) Brown, J. C.; Bass, H. E.; Thompson, D. L. *J. Phys. Chem.* **1977**, *81*, 479.
- (28) Huebert, B. J.; Martin, R. M. *J. Phys. Chem.* **1968**, *72*, 3046.
- (29) Gierczak, T.; Goldfarb, L.; Sueper, D.; Ravishankara, A. R. *Int. J. Chem. Kinet.* **1994**, *26*, 719.
- (30) Molins, R. F.; Setser, D. W. *J. Chem. Phys.* **1980**, *73*, 5666.
- (31) The spontaneous IR radiation from $\text{HCl}(\nu)$ and $\text{HBr}(\nu)$ is of the order of 10^{-60} s^{-1} , which makes these species negligible on our time scale of 0.26–1.85 s (see earlier remarks).

JP942805X